IOSUD - Universitatea Politehnica Timişoara
Şcoala Doctorală de Studii Inginereşti

Contributions on the fusion welding process of Duplex stainless steels

to obtain the scientific title of doctor (PhD) at
Polytechnic University of Timisoara
in the field of Ph.D. Program Materials ENGINEERING
made by ing. Dumitru – Sorin URLAN
scientific coordinator prof.dr.eng. Ion MITELEA

Chapter 1 Current Status of Research on the Welding Behaviour of Duplex Stainless Steels

1.2 Applications of Duplex Stainless Steels

Duplex Stainless Steels are an interesting alternative for numerous industrial applications, as they combine a high mechanical resistance with a high corrosion resistance. Among the main fields they can be used in there can be mentioned as example the following [18],[21], [23]:

- offshore oil and gas drilling platforms;
- see water desalination plants;
- chemical industry installations;
- equipments for food industry.

1.3 Welding Problems

The base material is delivered in form of sheets, tubes, bars, wires, castings or forgings, etc. either in hyper-hardened state (hardening treatment for bringing into solution), or in mechanic hammer-hardened state. For technological and economic reasons, the recommended welding procedures for these steels are:

- manual welding with coated electrode;
- WIG welding;
- MIG/MAG welding;
- welding with tubular rod;
- arc welding;
- plasma welding.

Nevertheless, the plasma welding or WIG welding processes without fillers shall be avoided. The WIG process is recommended for welding the root layer when welding only one side, such as in case of tubes, for example, where the manual welding with coated electrodes shall be used for the filler layers.

The ferrite content in the weld depends on the chemical composition of the selected filler and on the values of the process parameters. Different precipitation reactions may occur in the settled metal and in the heat-affected zone (HAZ) during welding. Precipitations shall occur almost exclusively in the ferrite, because of its high content of Cr and Mo, of high diffusion, as well as of the more reduced solubility of N in this phase. The most important two phases are the Sigma-Phase, rich in Cr and Mo, respectively the nitrides. The Sigma-Phase appears after prolonged high temperatures exposures and causes fragility and decrease in the corrosion resistance of the material. The nitrides affect the corrosion resistance and may be found especially in the zones with high ferrite content. The base materials having a high content of N

are less sensitive to nitride precipitation in HAZ, as N initiates the austenite formation and hinders in this way the nitrides formation.
These precipitation phenomena manifest themselves by decreasing the HAZ tenacity, by increasing the sensibility to post-weld cracking and by reducing the corrosion resistance. These problems can be avoided by focusing on the maintenance of the reached peak temperature for a minimum time during the welding procedure, by limiting the linear energy and the temperature between two successive passes.
In simplified terms there can be said that it is necessary to limit the highest temperature used for welding and the temperature between consecutive layers, in order to prevent the occurrence of Sigma-Phase, respectively that it is necessary to limit the lowest temperature, in order to avoid nitride formation.
Compared to the welded joints of austenitic stainless steels, the following defects may occur when welding the Duplex stainless steels:

- a more reduced penetration, determined by the high content of nitrogen (fig.1.8);
- a slightly increased tendency to form porosities and slag inclusions (fig.1.9);
- the arc stability, the arc fluidity and control are slightly more reduced.

1.4 Objectives of the PhD Theses

The difficulties reported for welding Duplex stainless steels required the performance of extensive experimental researches which should aim at fulfilling the following objectives:

- The advisability of performing some welded joints of X2CrNiMoN22-5-3 stainless steel by using the pulsed MAG welding procedure and of some manual electric arc welded joints between two dissimilar steels (low-alloy steel 13CrMo4-5 and Duplex stainless steel X2CrNiMoN22-5-3).

- The optimization of thermal condition parameters for the welding process, which should ensure a welding microstructure built-up of austenite and ferrite, the ferrite proportion being less than the one present on in the base metal; at the same time, the precipitation of some inter-metallic phases in HAZ, which might affect the tenacity characteristics, is to be avoided.

- The selection of some fillers compatible with the base metal, which should lead to obtaining a settled metal having favourable usage characteristics; thus, there has been decided to use a rod, E 2209, for joining similar materials and for using a coated electrode, E 309L, for dissimilar joints (Duplex steel + low-alloy steel).

- The quality evaluation of “black-white” welded joints by investigating the fine and the microscopic structure and by mechanical trials, establishing the guidelines to be taken into consideration in order to avoid the possible defects in a particular case of joining such steels.

Chapter 2. Researches on Pulsed MIG/MAG Welding Procedure

2.4 Experimental Procedure

LUC 500 Aristo welding source is part of the category of modern welding sources with inverter. It is built in modular system, is programmable, has a Siemens microprocessor and can be connected to the PC.

2.5 Used Materials. Establishing the Synergic Welding Program

Initial welding conditions:

- definition of jointing: **homogenous**

a. base metal:

Duplex stainless steel plates, s = 12 mm having the chemical composition mentioned in Table 2.2;

Tab.2.2 Chemical composition of the Duplex stainless steel plate X2CrNiMoN22-5-3, %mass

C, %	Si, %	Mn,%	P, %	S, %	Cr, %	Ni, %	Mo, %	N, %
0,021	0,79	0,82	0,019	0,021	22,34	5,61	3,1	0,14

- type of welded joint: butt seam penetration;
- weld thickness: 12 mm
- welding position: horizontal PA.;
- welding technique: pulsed MAG welding procedure;
- filler: rod E 2209-16 (according to AWS A5.4) ;
- electrode wire diameter: d_s = 1,2mm;
- shielding gas: Cronigon 2 (97,5 % Ar + 2,5 % CO_2), Linde;
- gas flow: 18 l/min.;
- welding direction: to the left;
- angle of the electrode wire: 85°;

The wielding was carried out in horizontal position, in the position PA/SRENISO 6943/2000. The welding joint preparation and the positioning of the components is presented in figures 2.11and 2.12. A butt welding with access from one side has been carried out.

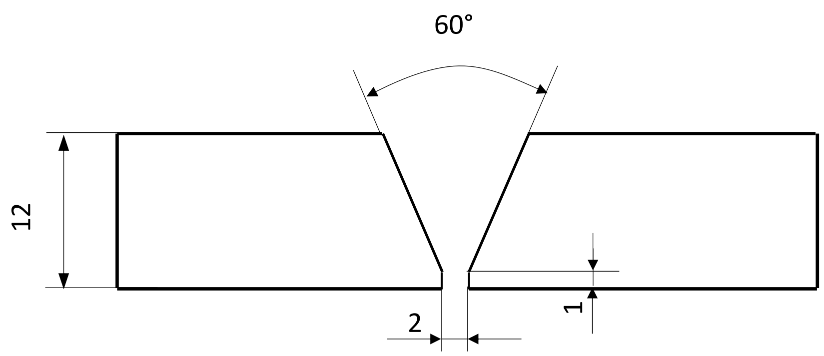

Fig. 2.11 Welding joint form and dimensions

Fig. 2.12 Position of the components to be welded

Figure 2.13 presents the position of the components and of the welding gun.

Fig. 2.13 Welding components and gun

Experimental researches focused on studying the influence of linear energy on the structural modifications occurred in the welding joints areas. 3 welding sample sets have been done for this purpose, each of them with different linear energies and in each case using 2 different welding technologies, one for building the root layer and one for building the filler layers.

2.6 Conclusions

1. The carrying out of the welding joints by pulsed MAG welding procedure, of Duplex stainless steel plates having a thickness of 12 mm by using as filler the E 2209 – 16 wire with a diameter of Ø 1,2 mm and Cronigon 2 shielding gas, Q = 18 l/min., requires a welding technology for the root layer and another technology for the filler layers.
2. In order to avoid perforation and melt metal leakage, the root layers has been done by using a lower linear energy, of 6,9 kJ/cm, respectively the following welding parameters:
   - wire feed speed, 5 m/min.;
   - average welding current, 116 A;
   - electric arc voltage, 20 V;
   - welding speed, 20 cm/min.

3. The optimal values of the technological welding parameters for the filling passes experimentally settled are:

- wire feed speed, 8 – 9,5 m/min.;
- welding current, 180 – 230 A;
- arc voltage, 28 – 30 V;
- welding speed, 30 - 20 cm/min.;
- linear energy, 10 – 20,7 kJ/cm.

4. The linear energy variation between 10 and 20,7 kJ/cm when filling the welding joint, by reducing the welding speed or by increasing the current, allowed us to obtain a root layer with no defects, with metallic continuity, and a surface with no defects of the type marginal denting.

Chapter3 Investigations on the Structure and Mechanic Properties of Homogenous Welded Joints of Duplex Stainless Steels

3.1 Macrographic Examinations

The macrographic images of some cross-sections through the welded joints carried out by using constant linear energy for the welding joint and variable linear energy for the filler layers are given in Figure 3.1.

- a -

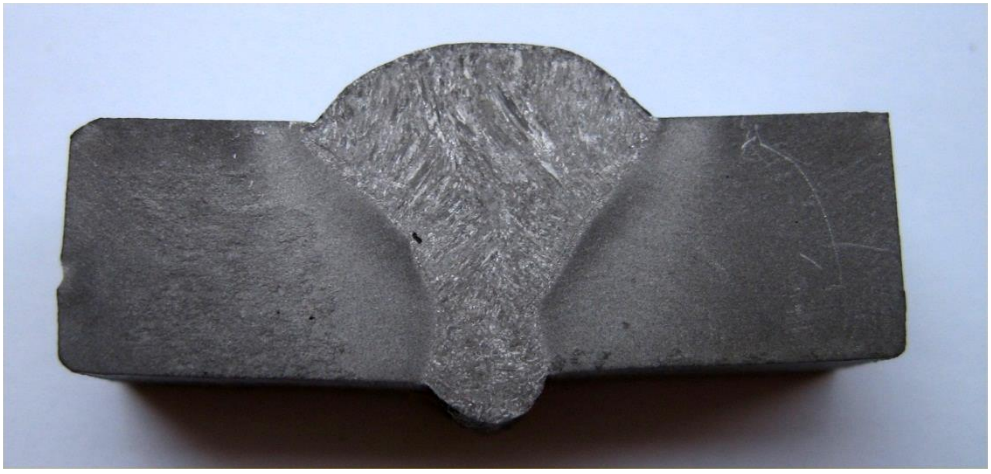

- b -

-c-

Fig. 3.1 Macrographic images of some sections through the welded joints:

a – E_l welded joints = 6,9 kJ/cm; E_l filler layers = 10 kJ/cm;

b - E_l welded joints = 6,9 kJ/cm; E_l filler layers = 15 kJ/cm;

c - E_l welded joints = 6,9 kJ/cm; E_l filler layers = 20,7 kJ/cm.

Chemical reagent: ferric chloride 10 cm^3; hydrochloric acid 30 cm^3; ethyl alcohol 120 cm^3

3.2 Micrographic Examinations

The representative microstructures of the welded joint areas are shown in figures 3.2 and 3.3. There can be noticed that the base metal (figure 3.2) has a structure composed of approx. 52 % austenite and 48 % ferrite (determined with a Fischer feritscope), the settled metal has a structure with dendritic orientation (figure 3.3), its morphology depending on the particularities of the thermal cycle of welding. In the welding joint area the thermal cycle is the most severe, the cooling speed is rather high and the austenite from ferrite formation time is reduced. A superposition of thermal cycles occurs by settling the subsequent layers, the welding portion in the joint is heated again and, as a consequence, it favours the re-crystallisation of ferrite grains on one hand and the initiation of secondary phase precipitation phenomena on the other hand. Both phenomena are specific to both welding and thermal influenced area.

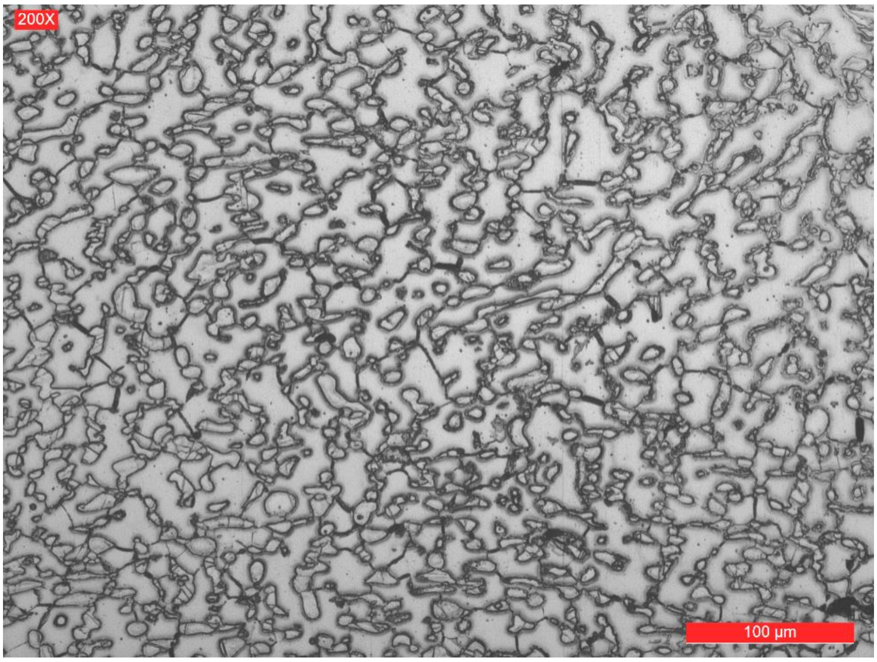

Fig. 3.2 Base metal microstructure

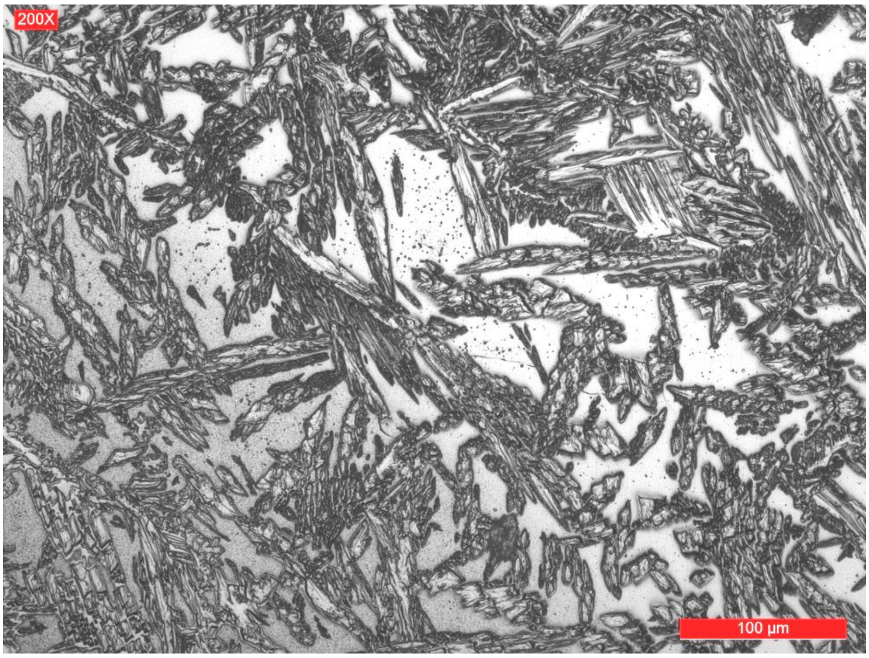

Fig.3.3 Root layer microstructure

The ferrite content of the settled metal must normally correspond to the ferrite index FN 30 - 100 (22 – 70 %)[69],[89]. The ferrite index of the settled metal has been asserted as being of FN 32 – 38 (24 – 28 %). ny transferring the $Cr_{ech.}$and $Ni_{ech.}$values specific to the base metal and to the filler to the WRC diagram – 92 [69] in fig.3.5, and by taking into consideration the dilution degree value.

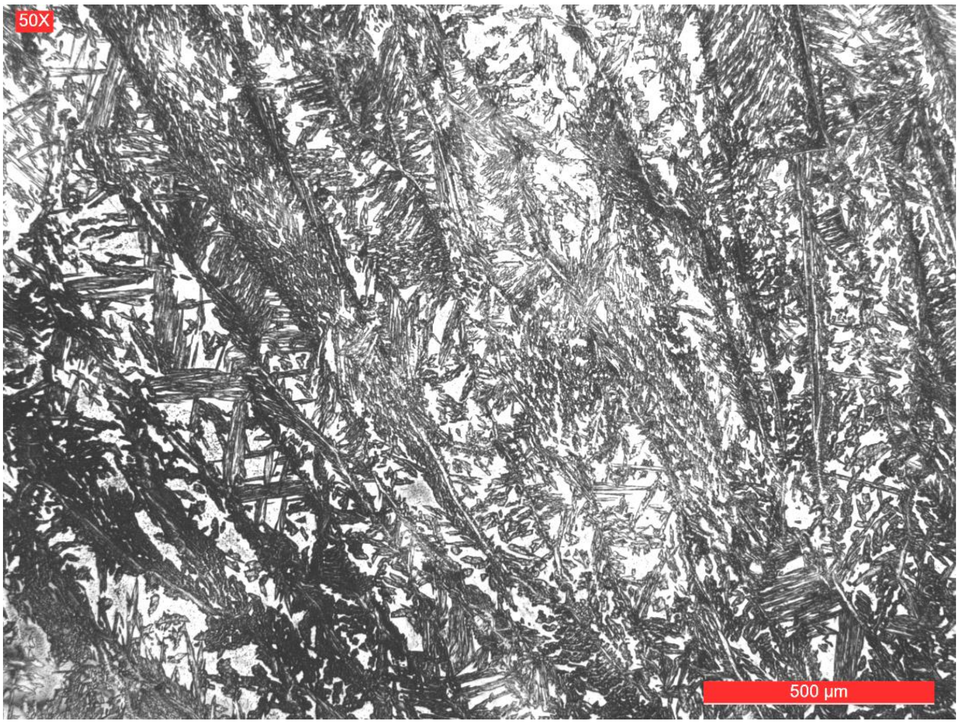

- a –

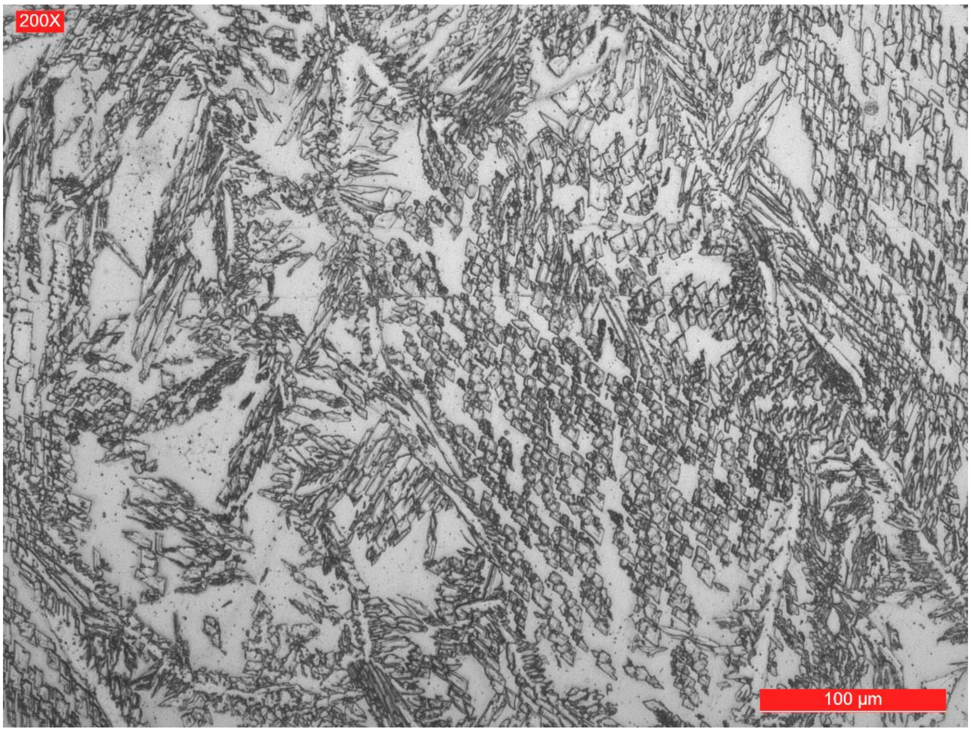

- b -

Fig.3.4 Microstructure of the last pass when barring out the welding with a lineal energy E_l = 15 kJ/cm: **a – x 50; b – x 200**

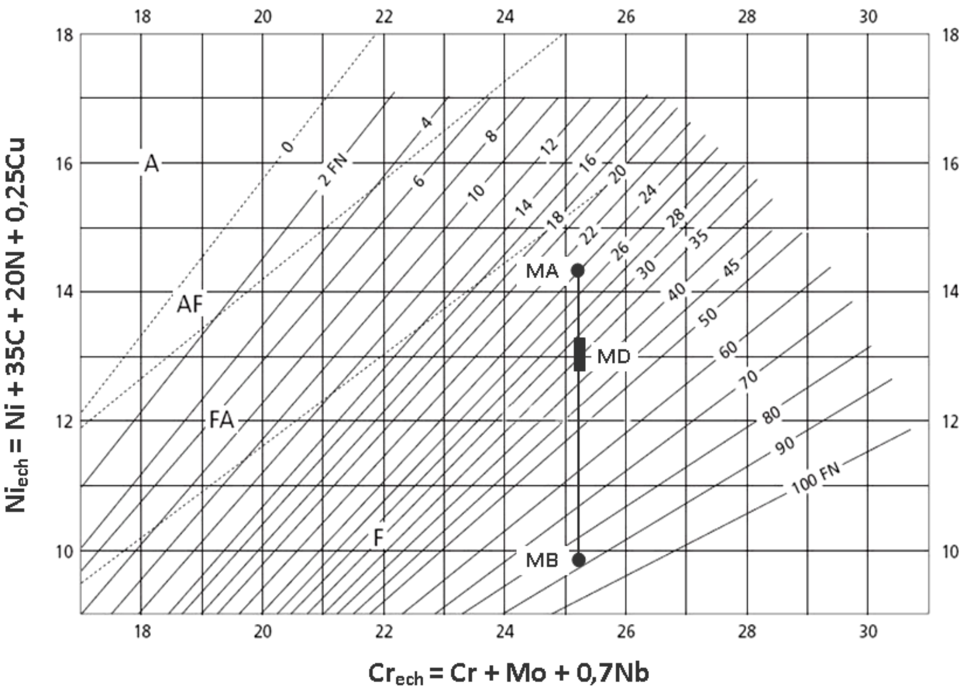

Fig.3.5 Prediction of the ferrite index

A predominantly ferritic structure occurs in the area from the heat affected zone (HAZ) adjacent to the fusion line (Figure 3.6).

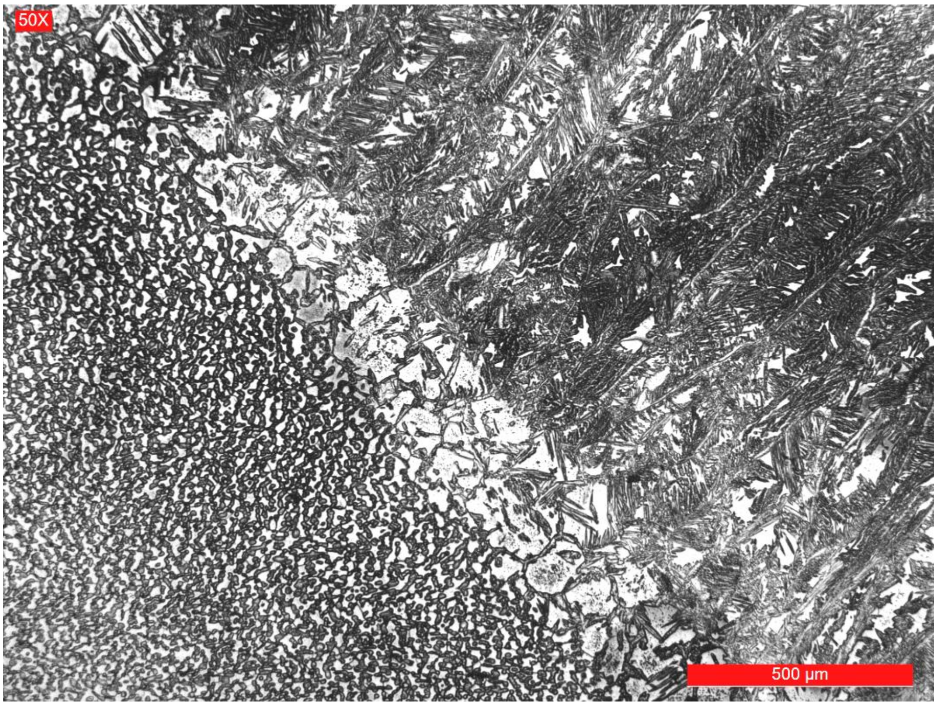

- a -

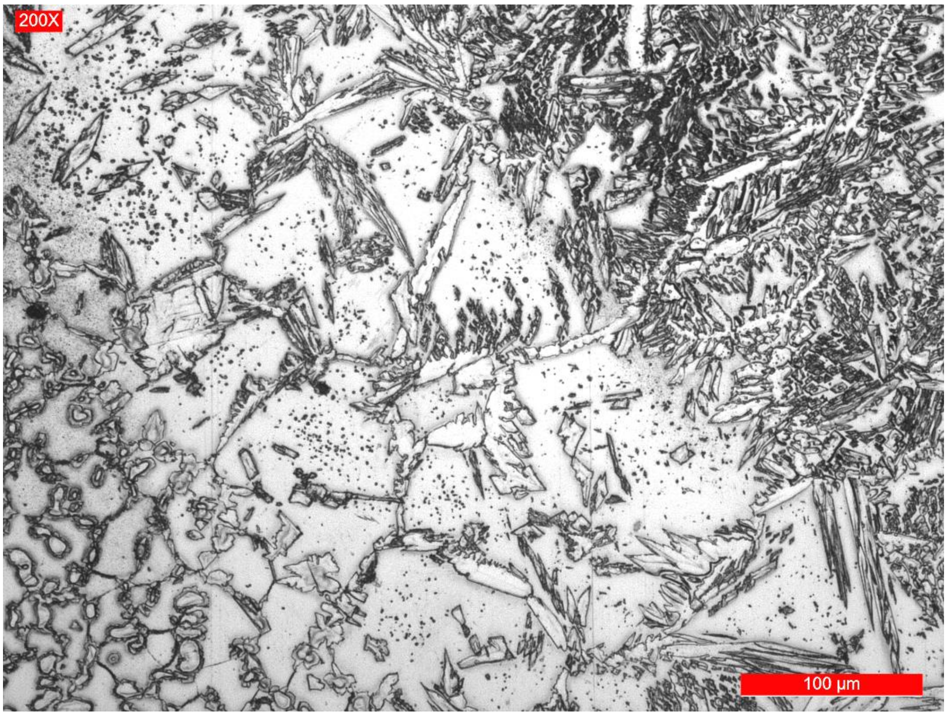

- b -

Fig.3.6 Microstructure of the welding interface – HAZ when welding with a linear energy: E_l = 15 kJ/cm: **a – x 50; b – x 200**

The limitation of the linear welding energy to the values settled as optimal, together with the supplementary alloying with nitrogen decrease the tendency of grains growing and of σ phase precipitation. At the same time there can be noticed the precipitation of some fine nitride particles, Cr_2N, having the aspect of plates and of carbides $M_{23}C_6$[8],[9],[40]. The higher the linear energy, the lower the quantity of ferrite in the welding and in HAZ and the higher the danger of inter-metallic phase formation. Moreover, the presence of nitrogen as alloying element slows down the increase in dimension of the crystalline grains and, as a consequence of its high solubility in austenite, the proportion of precipitated nitrides will not be very high. A structure with a higher proportion of ferrite may decrease the tenacity at low temperatures, while a structure with a too high quantity of austenite affects both the characteristics of mechanical resistance and of corrosion resistance under voltage in environments containing chlorides. The hot cracking sensibility is reduced precisely because of the higher concentrations of Ni and of N. At the same time, the cold cracking resistance of the austenite-ferrite welding and of the highly ferritized area in the HAZ is high, although in the austenitic regions situated in the vicinity of the ferritic area a significant quantity of hydrogen can be deposited. In order to eliminate the risk of cold cracking it is recommended to choose some welding materials with low hydrogen content and to apply a preheating at about 150 ˚C.

3.3 EDX Analysis

During the solidification of the molten metal bath, the cooling speeds specific to arc welding are so high, that they segregate the alloying elements. In addition to that, the transformation of ferrite into austenite is associates to a redistribution of Cr, Ni, Mo and N between the two phases (Table 3.1). These data demonstrate that ferrite becomes richer in Cr, Mo and poorer in Ni, N. As a result, the chemical composition of ferrite presents more Cr and Mo in the alloy as compared to the average composition of the welding and of austenite.

Tab.3.1 Variation of the alloy elements concentration in the welding, in case of a linear energy,

E_l = 15 kJ/cm

Phase	Cr, % mass	Ni, % mass	Mo, % mass	N, % mass
Ferrite / Ferrite	21,61 – 23,83	5,40 – 6,22	2,62 – 3,35	< 0,052
Austenite/ Austenite	19,92 – 21,5	6,31 – 8,70	2,51 – 2,98	0, 31 – 0,58

Table 3.2 and figures 3.7 and 3.8 show the variation of Cr, Ni, Mo concentration in different areas of welded joints carried out with a linear energy, E_l of 6,9 kJ/cm for the welding joint and of 15 kJ/cm for the filler layers.

Tab.3.2 EDX investigations on the areas of welded joints

Welded joint area	Phase	Cr, % mass	Ni, % mass	Mo, % mass
Weld root	F / F	23,62	7,16	2,98
	A / A	23, 14	7,85	2,67
Heat affected zone (HAZ)	F / F	21,88	5,17	3,39
	A / A	20,76	5,83	2,87
Weld – middle zone	F / F	24,84	6,18	3,68
	A / A	22,60	8,55	2,47
Weld –exterior zone	F / F	23,71	7,20	2,73
	A / A	23,42	7,72	2,54
Base metal	F / F	23,18	4,08	3,29
	A / A	19,47	7,16	2,43

Such variations in the concentration of alloying elements in the weld and in the heat affected zone (HAZ) are based both on the transformation reactions and on the precipitation reactions that took place during a large range of temperatures of between 1300 ˚C and approx. 300˚C. It is underlined the fact that the degree of alloyed elements redistribution strongly depends on the global thermal cycle specific to the welding operation. Because of the high temperatures reaches in the vicinity of the joining area, a transformation in solid state with austenite formation takes place during the subsequent cooling, although the heat affected zone becomes predominantly ferritic at the maximal temperature reached during welding. A redistribution of the alloying elements comparable with that noticed in the weld will consequently take place.

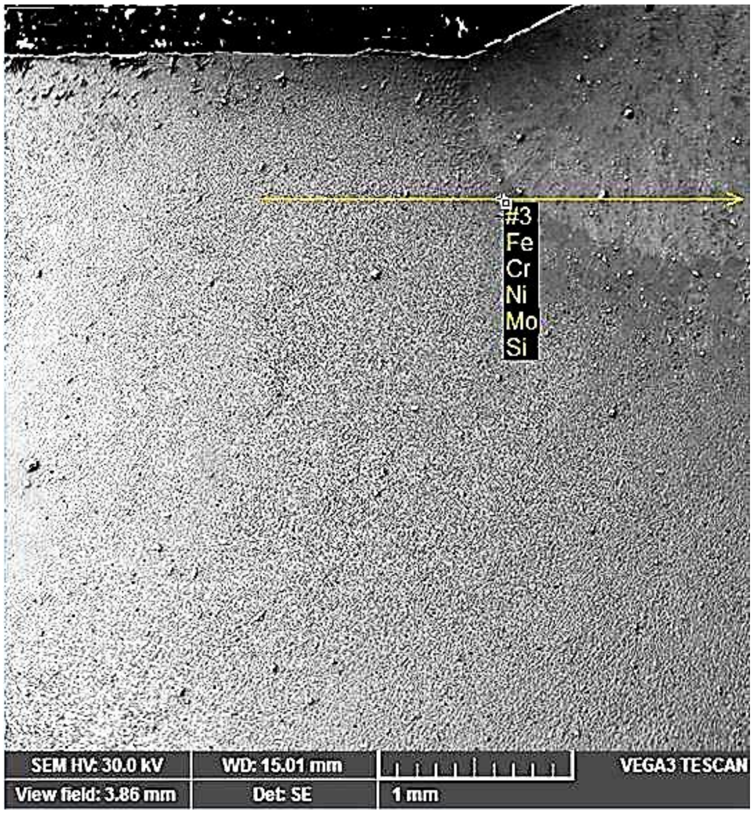

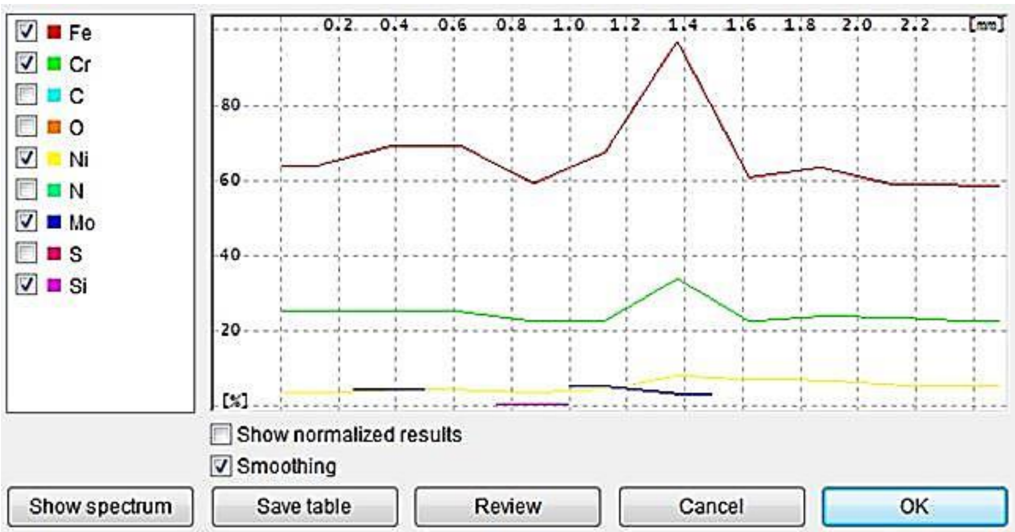

Fig.3.7 Linear variation of Fe, Cr, Ni, Mo and N concentration present at the last passing through the settled layer with $E_l = 15$ kJ/cm

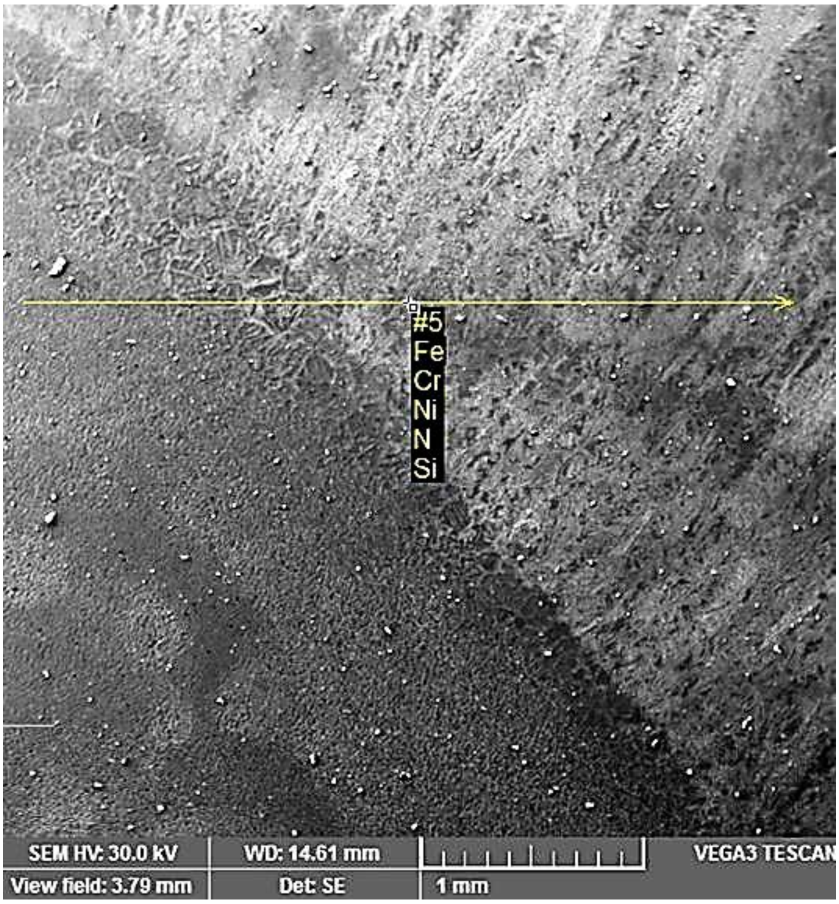

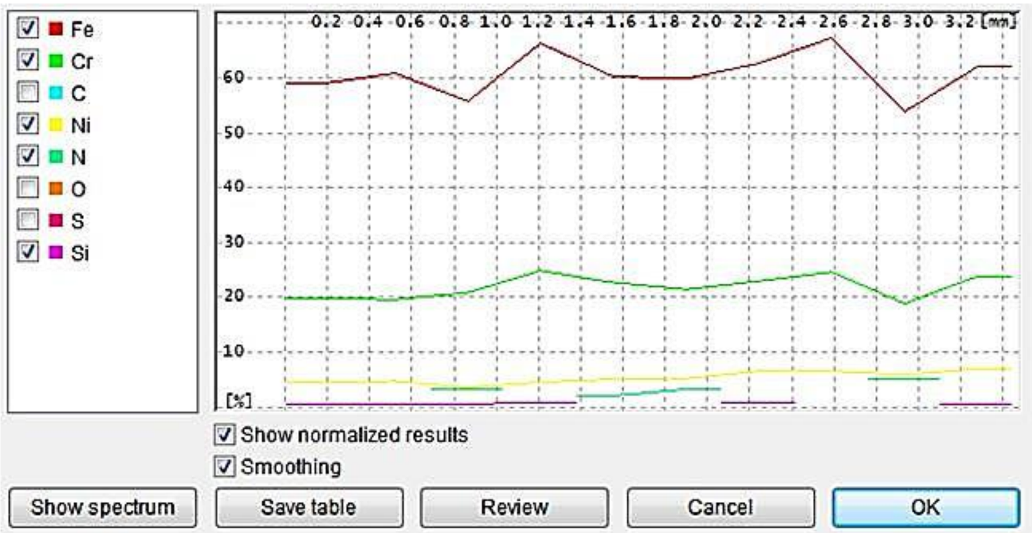

Fig.3.8 Linear variation of Fe, Cr, Ni, Mo and N present in the middle region of the settled layer, at E_l = 15 kJ/cm

3.5 Mechanic Properties of Welded Joints

In order to asses the behaviour of the material at extraordinary mecanical efforts, there have been carried out both hardness tests and static traction tests.

The hardness is the mechanical characteristic most sensible to structural modifications that occur in the material. Figures 3.17 and 3.18 show the hardness gradient curves on the cross-section of welded joints at a distance of 2 mm from the exterior surface, respectively from the point the root starts.

If in the base metal the obtained microhardnes values are HV 0.3 = 260...280 daN/mm^2, the root layer has values of HV 0.3 = 290...320 daN/mm^2, and the last filler layer settled has values of HV 0.3 = 280...300 daN/mm^2.

Theese microhardness variations are due, on one hand, to the changes in the chemical composition of the two structural phases (ferrite and austenite) in the root layer and in HAZ, and on the other hand to the dendritic character of the microstucture, irrespective of the global thermal cycle specific for each part of the welded joint.

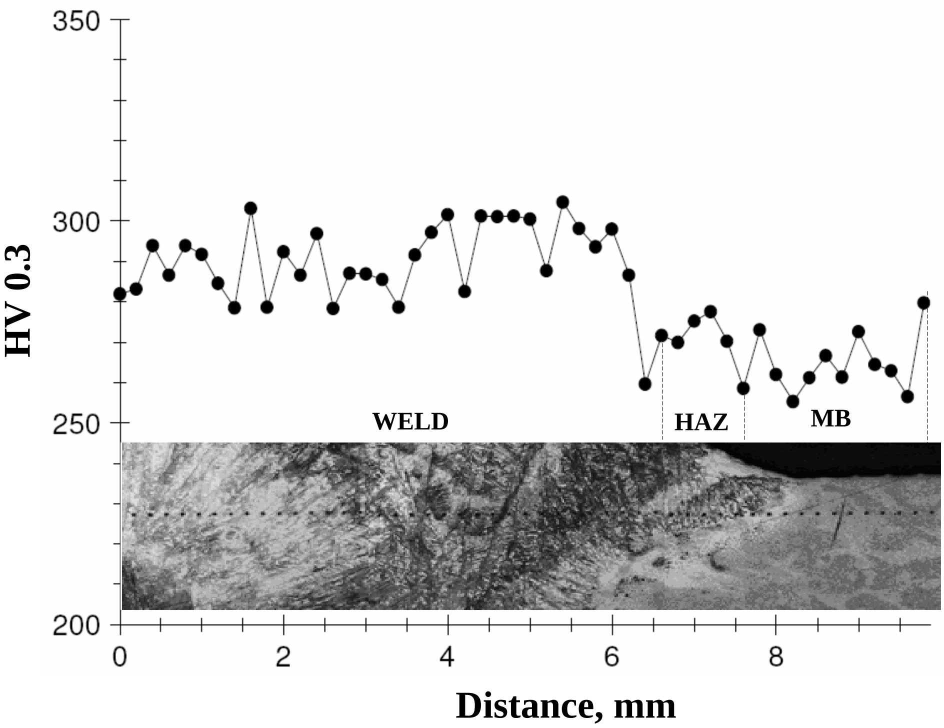

Fig.3.17 Variaţia microdurităţii şi a microstructurii pe secţiunea transversală a îmbinării sudate, E_l= 15 kJ/cm

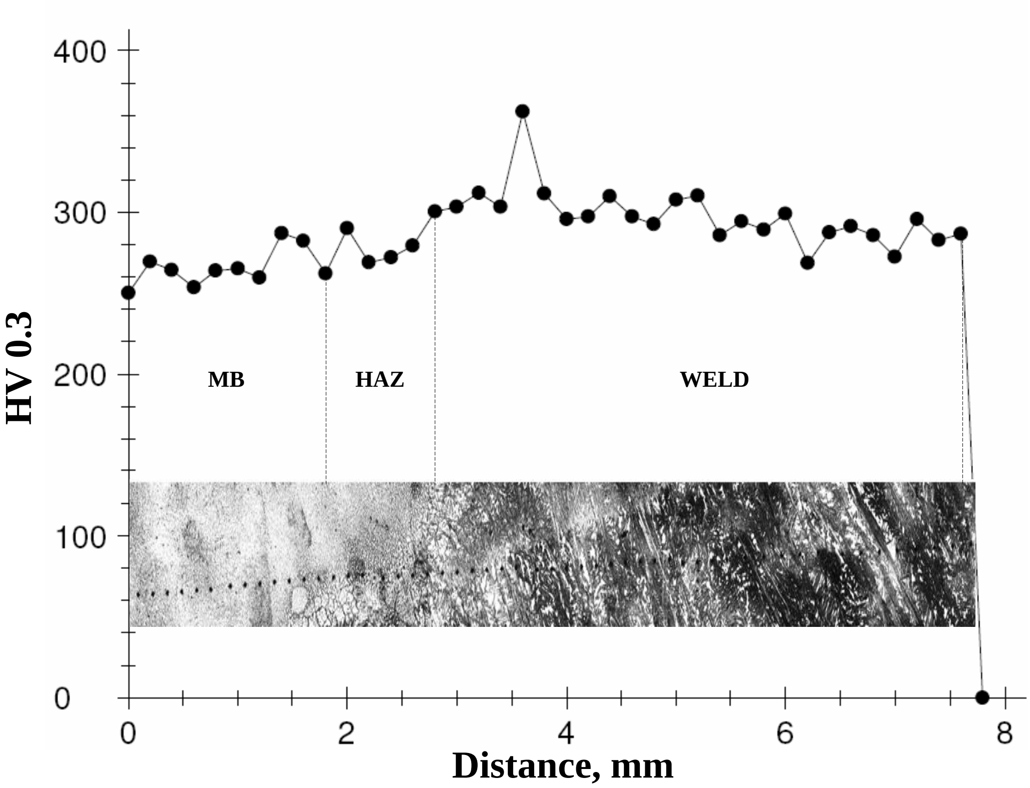

Fig.3.18. Variaţia microdurităţii şi a microstructurii pe secţiunea transversală a îmbinării sudate în zona stratului de rădăcină, E_l= 6,9 kJ/cm

The impact bending dynamic trials highlight the tendency of a material to fragile breakage. Notched bars having a V form middle notch have been used for the experiments. They were preferred to those having a U form notch, because the assessed breaking energy is mainly attributed to crack propagation. According to the valid norms, the bending characteristic of these notched bars confine themselves to the energy consumed for breaking, noted KV and expressed in J. In order to assess the tenacity characteristics trials have been carried out of the settled metal, at temperatures ob between +20 and – 40 ^{0}C. The bars' notch was oriented on the direction of the settled metal thickness.

Some of the notched bars have been tested in welded state, without subsequent thermal treatment, and other samples have been submitted to a thermal hardening treatment for bringing into solution, after a thermal regime similar to the one applied to the notched bars for static traction tests.

In order to make a comparison there have also been tested notched bars having the notch in the base material. The results delivered by these tests are shown in Table 3.21., and based on them energy variation curves have been drawn depending on the trial temperature (Fig.3.21).

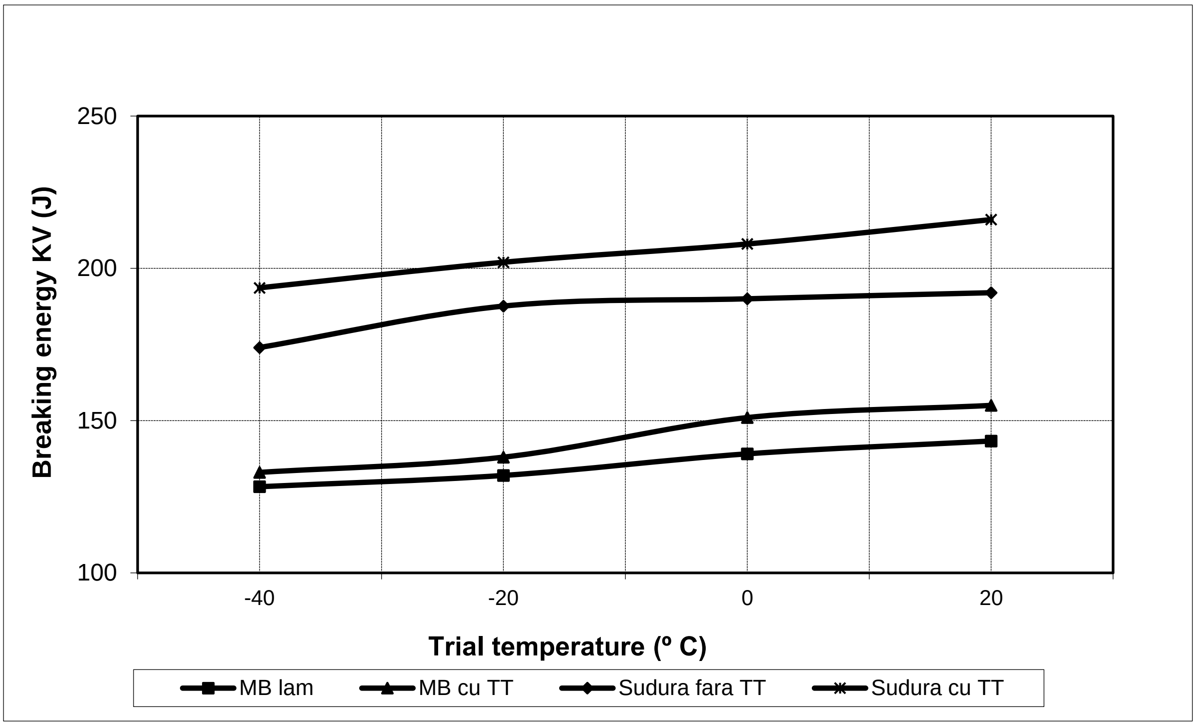

Fig.3.21 Breaking energy variation according to the trial temperature

Chapter 4 Possibilities of Welding Dissimilar Materials

4.3 Experimental Procedure

Initial welding conditions:

- definition of jointing : **heterogenic**

  a. base metals: Duplex stainless steel sheets with low alloy steel sheets 13CrMo4-5, s = 8 mm;

- joint type: butt seam penetration ;
- weld thickness: 8 mm
- welding position: horizontal PA.;
- welding technique: manual, arc welding;
- filler material: wire E 309MoL-16 (acc. AWS A5.4) ;
- electrode diameter: d_s = 2,5mm.

The welding was carried out in horizontal position, PA/SRENISO 6943/2000 position. The joint preparation, the positioning of the components and the outside appearance of the executed joint are presented in Figures 4.1, 4.2 and 4.3. A butt seam penetration joint was carried out, with the access from the side.

The welding was carried out with 3 passes, 1 deep pass and 2 filling passes with the following technological welding parameters:

- average welding current, 85 A;
- arc voltage, 26 - 28 V;
- welding speed, 17-19 cm/min;
- linear energy, 7.5 – 7.8 kJ/cm;

In accordance with Figure 4.2, the joint was filled by 2 passes, and the temperature between two consecutive passes was limited to 200°C.

Tab. 4.1 Chemical composition of the used materials

Type of material	Chemical composition, % mass									
	C	Mn	Si	P	S	Cr	Ni	Mo	Cu	N
Base metal, X2CrNiMo22-5-3	0,026	1,86	0,74	0,019	0,014	22,2	5,10	2,94	-	0,16
Base metal, 13CrMo4-5	0,11	0,59	0,32	0,021	0,022	0,94	-	0,51	0,18	-
Filler material, E309MoL-16	0,024	1,06	0,75	0,019	0,015	22,96	12,80	2,35	-	-

Tab. 4.2 Equivalent chrome and equivalent nickel values

Type of material	Equivalent Chrome- $Cr_{ech.}$,%	Equivalent nickel - $Ni_{ech.}$,%
Base metal, X2CrNiMo22-5-3	25,14	9,21
Base metal, 13CrMo4-5	1,93	3,595
Filler material, E309MoL-16	26,435	14,05

4.5Macro- and Micrographic Analysis of Welded Joints

The macrographic image in Figure 5 shows the shape and width of the characteristic areas of the welded joints, as well as the absence metal continuity defects of crack-type, slag deposits, pores, etc.

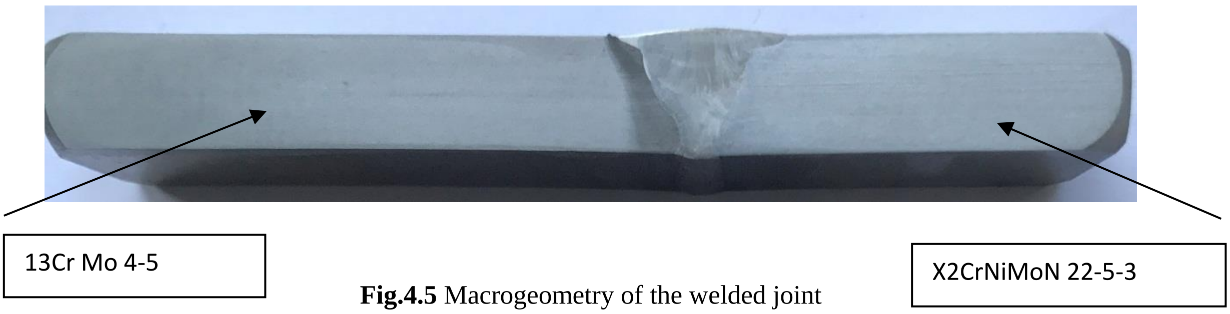

Fig.4.5 Macrogeometry of the welded joint

The results of metallographic tests (Figures 4.6 to 4.9) performed on some relevant samples collected perpendicularly on the longitudinal axis of the weld confirm the predictions given by the Schäffler model. Thus, the welded seam shows a dendritic structure comprising austenite and a ratio of 12 – 16% of ferrite δ (Figure 4.6) preventing hot cracking. The basic Duplex stainless steel shall show a microstructure made of approx. 40 – 42 % austenite and 58 - 60 % ferrite (Figure 4.7a) in the overheating subzone of the heat affected zone (H.A.Z.). The solidification process sets in on the walls of the crystals of both basic metals that remained in a solid state, and the increase size of the grains is epitaxial. In the area adjacent to the Duplex stainless steel fusion line, the heat from welding led to solution forming of secondary phase particles and a slight increase in the size of crystal grains (Figure 4.7a).

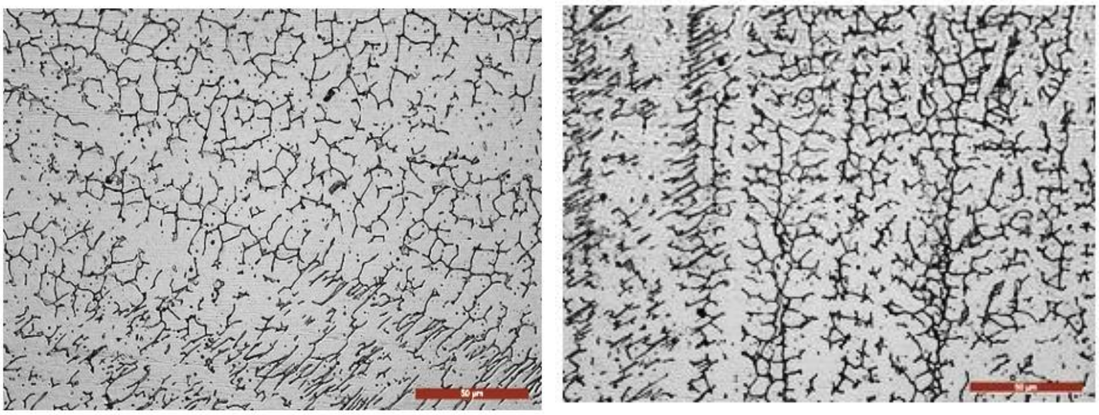

- a -- b -

Fig. 4.6 Welded seam: a – basic layer; b – filler layer

By contrast, the overheating subzone of the heat affected zone (H.A.Z.) of the steel with the point of transforming in solid state is characterized by a heterogeneous ferritic-bainitic-martensitic microstructure (Figure 4.7a) mainly determined by the heterogeneous characteristics of the dilution. The presence of alloy elements (Cr, Mo), generating carbons, increases the value of the critical points Ac_1 and Ac_3, delaying the diffusion transformations during the austenitization process. Therefore, a heterogeneous austenite will be obtained in the H.A.Z., which, by quick cooling, will lead to the local formation of martensitic colonies with high carbon content. (Figure 4.7a).

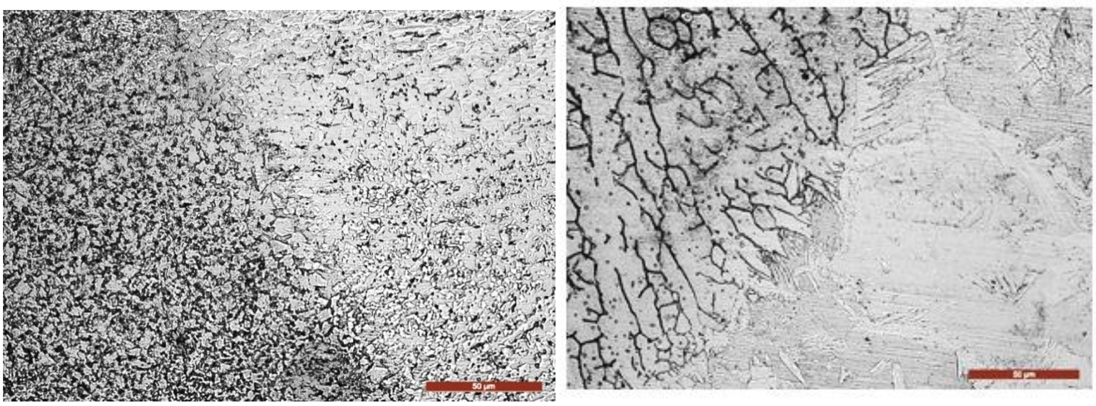

-a- -b-

Fig. 4.7 MD – MB interface; a – weld – low alloyed steel; b – weld –Duplex stainless steel

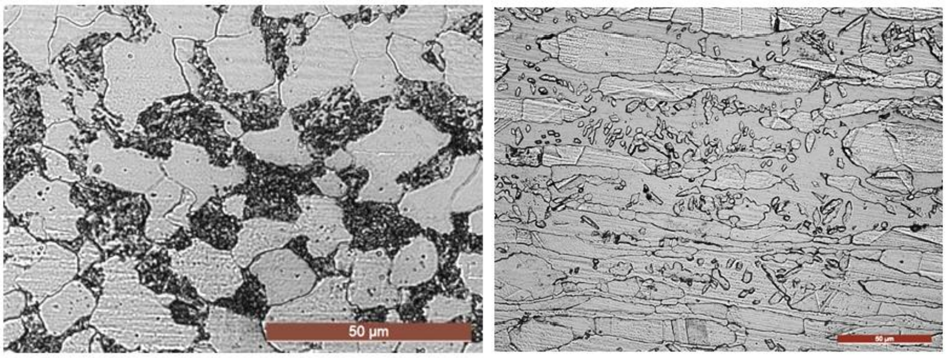

-a- -b-

Fig. 4.8 Basic metals: a – low alloyed steel; b – Duplex stainless steel

The two basic metals that are not affected by the welding process have a microstructure made of alloyed ferrite + bainite + pearlite (Figure 4.8a –13CrMo4-5 steel), respectively austenite + ferrite (Figure 4.8b –X2CrNiMoN22-5-3 steel).

Based on these results there can be concluded that micro-structural constituents of different nature are formed at the V form joints, because of the different degrees of dilution obtained on the cross-section of the weld.

According to a first estimate, the transition zone of such welded joints consists of the following three structural sections:

H.A.Z. of the 13CrMo 4-5 steel / the martensitic network / austenitic-austeritic-ferritic settled metal

The area of martensitic structure starts straight on the fusion line and stretches into the settled metal. One of the causes that led to the occurrence of the martensitic phase was the turbulences in the settled metal caused by the electric arc pressure, so that also isles with such a micro-structures often appear, the last ones being favoured in case of manual welding [24].

Chapter 5. Corrosion Resistance of MAG Welded Joints in Pulse Current from Duplex Stainless Steels

The assessment of the welded joints corrosion behavior after the application of the quenching thermal treatment was done by linear voltammetry. This method consists in measuring the current that develops in an electrochemical cell by applying a voltage at the circuit terminals between two potentials, one positive maximum potential and the other a negative maximum potential, with a constant variation gradient. For testing, a three-electrode corrosion cell was used: working electrode (sample), reference electrode (calomel saturated electrode), and counter-electrode (platinum electrode). The potential was changed with a scanning rate of 0.16 mV / s. The potential scaling range varies depending on the sample, and can be tracked on each graph separately. For testing, the potential range was -500mV and + 1500mV.

The mode of operation is shown in Figure 5.7 and involves the application of a voltage between the working electrode and the reference electrode and the measuring of the current generated between the sample and the auxiliary electrode.

The plant used (Fig.5.8) consists of the SP-150 potentiostat and the electrochemical corrosion cell of BioLogic Science Instruments.

Fig. 5.8 Voltametric cyclic plant SP150

A 3.5% sodium chloride solution was used as a test medium. The area of the sample surface that was in contact with the corrosive medium was 1 cm^2. On the basis of the measurements, the polarization curves presented in comparison in Figures 5.9a and 5.9b were drawn, and the potential, the current and the corrosion rate were determined (Table 5.3) after the tangents were drawn between the cathode and anodic branches.

Table 5.3 Values resulting from potentiostatic tests

Origin of the sample	Corrosion Parameters		
	i_{corr}, nA/cm^2	U_{corr}, mV	V_{corr}, nm/year
Base metal, MB	44.66	-141.2	1532
Welding without further thermal treatment	12, 52	21,6	1135
Welding with further thermal treatment	3.74	-135,7	775
ZIT without further thermal treatment	630.48	-75.5	10231
ZIT with further thermal treatment	75.07	12.4	2141

Chapter 6 Final Conclusions and Original Input. Future Research Directions

5. **Micrographic investigations** and **X-ray diffraction analyzes** conducted in areas including the entire welded joint have revealed the occurrence of transformation and precipitation reactions that are mainly determined by the chemical composition and local microstructures generated by the induced thermal cycle. For the welding conditions used, the base metal consists of approx. 52% austenite and 48% ferrite, and welding is consisting in approx. 26-32% ferrite

and 68-74% austenite, the ferrite content decreasing as we move from the surface to the root layer.

6. The **primary and secondary crystallization** process of the molten metal bath is manifested by a segregation of the alloying elements and a redistribution of them between the two phases, ferrite and austenite.

Following the high temperatures reached in the area adjacent to the fusion line, with a **small thickness of approx. 120 - 160 µm**, its microstructure becomes predominantly ferritic, and the subsequent cooling triggers the partial transformation into austenite.

7. The execution of **the root layer** with a linear energy of 6**.9 kJ /cm** and the **filling layers** with its values of **10 - 20 kJ /cm** are preventing the phenomenon of weld cracking and are limiting the precipitation of fragile intermetallic phases in the welded joint areas.

8. The results of the **mechanical tests** prove the good compatibility between the base metal and the deposited metal, and the application of thermal treatment after welding (hardening for solution) facilitates an increase in breaking strength of approx. 18% and in the breaking energy with approx. 8 - 12%.

9. X-ray energy dispersion spectra, along with the results of quantitative chemical analyzes in microvolumes of material, have shown that cross-sections of welded joints show variations in narrow limits of concentrations in alloying elements determined essentially by the particularities of the solidification process of the bath fused metal.

10. Applying the **post-welding hardening** thermal treatment **for the solution** to the technological parameters specific for the base metal (1060˚C / water) causes the structural balance to be restored and a uniform distribution of alloying elements (Cr, Mo, Ni) between ferrite and austenite in both welding as well as in ZIT welded joints.

11. Elucidation of some **phenomenological phenomena** occurring in the manual arc welding of the stainless steel Duplex with low alloyed steels, which essentially concern the structural transformations triggered in the heterogeneous welded joint, the interaction between the material of the components, the work contributing to the modification of the chemical composition of the molten bath, and to the nature and size of the transition zone between the solid alloy and the molten bath, the effect of the welding parameters on the morphology of the molten zones.

12. As a result of the relatively high **13CrMo 4-5 steel hardness** due to carbides-generating alpha-alloy elements (Cr, Mo) in the heat-affected area, a non-homogeneous austenitic is obtained which, by high-speed cooling leads to the localized formation of some **martensite colonies** having high carbon content and hardness values of HV = 260 ... 270 daN / mm^2.

Bibliography

18. Coussement C. - Application industrielle de l'acier inoxydable duplex dans l'industrie pétrochimique - endommagement d'un serpentin de réacteur en duplex. Revue de la soudure, 1994, 2, pp. 52-55.

21. Dhooge A., a.o. - Duplex stainless steels. Applications, advantages and limitations. Revue de la soudure, 1997, 1, pp 63-70.

32. Jiang Y., Tan H., Wang Z., Hong J., Jiang L., Li J. - Influence of Creq/Nieq on pitting corrosion resistance and mechanical properties of UNS S32304 duplex stainless steel welded joints, Corros Sci, 70 (2013), pp. 252–259

33.Jian L., Yaling D., Longfei L., Xiaoming W. - Microstructure of 2205 duplex stainless steel joint in submerged arc welding by post weld heat treatment. J. Of Manufacturing Processes, Vol.16, Issue 1, 2014, pp. 144 – 148

40. Lippold J.C., Kotecki D.J. - Weldability of stainless steels, Welding Metallurgy, John Wiley &. Sons, New Jersey (2005), pp. 230–253

44. Luo J., Liu D.J., Zhao G.J., Wang X.J., Ran H.Q. - Relationship between microstructure of fusion zone and mechanical properties of 2205 duplex stainless steel joint in double-sided submerged arc welding, Rare Metal Materials and Engineering, 40 (2011), pp. 369–374

72. Shaoning G., Junsheng S., Lingyu G., Hongquan W. - Evolution of microstructure and corrosion behavior in 2205 duplex stainless steel GTA – welding joint. J. of Manufacturing Processes, Vol. 19, 2015, pp. 32 – 37

75. Tan H., Wang Z., Jiang Y., Yang Y., Deng B., Song H. - Influence of welding thermal cycles on microstructure and pitting corrosion resistance of 2304 duplex stainless steels. Corrosion Science, 2012, 55, pp.368–377

80. Ureňa A., Otero E., Utrilla M.V., Munez C.J. - Weldability of a 2205 duplex stainless steel using plasma arc welding, Journal of Materials Processing Technology, 182 (2007), pp. 624–631

88. Young M.C., Chan S.L.I., Tsay L.W., Shin C.S. - Hydrogen-enhanced cracking of 2205 duplex stainless steel welds, Materials Chemistry and Physics, 91 (2005), pp. 21–27

96. xxx - How to weld duplex stailess steels. Avesta Welding, 2014, pp. 2 – 18

97. xxx - Practical guidelines for the fabrication of Duplex stainless steels. International Molybdenum Association, 2001, pp. 3 -39